Malaysian Journal of Chemistry, 2024, Vol. 26(3), 151-160
(Special Issue: *The International Conference on Advanced Materials & Sustainable Energy Technologies 2023*)

Highly Efficient Nonenzymatic Electrochemical Sensor for COD Measurement using ZnO/rGO

Norilhamiah Yahya*, Muhamad Zulhairi Sharil and Nur Afifah Mat Razali
Universiti Kuala Lumpur Malaysian Institute of Chemical and Bioengineering Technology, Lot 1988, Bandar Vendor, 78000 Alor Gajah, Melaka, Malaysia
*Corresponding author (e-mail: norilhamiah@unikl.edu.my)

This study presents the production and comparative analysis of electrochemical sensors designed for swift assessment of Chemical Oxygen Demand (COD) in lake water samples. Utilizing the hydrothermal method, Zinc Oxide/reduced Graphene Oxide (ZnO/rGO) nanocomposites were effectively synthesized. Examination of the X-ray Diffraction (XRD) patterns of the ZnO_1/rGO_1 nanocomposites illustrates the presence of hexagonal phase ZnO with a wurtzite structure. Field Emission Scanning Electron Microscopy (FESEM) images depict the integration of ZnO nanoparticles onto the rGO sheets. The Brunauer–Emmett–Teller (BET) analysis indicates a substantial increase in surface area and pore volume due to the presence of rGO, facilitating the unhindered movement of glucose and real lake water samples. Thermogravimetric Analysis (TGA) demonstrates the thermal durability of the synthesized electrode. Initially, sensor responses were assessed using glycerol as a standard analyte, followed by analysis of real lake water samples from the vicinity of Bandar Baru Bangi. The COD values obtained from the samples were compared against the standard dichromate method. Notably, the electrode crafted with the ZnO_1/rGO_1 nanocomposite exhibited superior electrochemical performance, with COD values closely aligning with those derived from the standard method within 95% confidence intervals. The developed ZnO_1/rGO_1electrochemical sensor stands as a promising candidate for COD electrochemical sensing in real lake water samples.

Keywords: Zno/rGO; electrochemical; COD; lake water sample

Received: January 2024; Accepted: March 2024

Water quality monitoring is of paramount importance for environmental sustainability and human health. Among the various parameters used to assess water quality, Chemical Oxygen Demand (COD) stands out as a critical indicator of organic pollution levels in water bodies [1]. Conventional methods for COD determination often require the use of hazardous chemicals such as potassium dichromate, mercury, and sulfuric acid [2]. These chemicals pose health and safety risks to laboratory personnel and contribute to environmental pollution during disposal. In recent years, electrochemical sensors have emerged as promising tools for water quality analysis due to their high sensitivity, selectivity, and real-time monitoring capabilities.

The emergence of electrochemical sensors employing nanomaterials has sparked considerable interest in environmental monitoring. Note that Zinc Oxide (ZnO) and reduced Graphene Oxide (rGO) are two such nanomaterials that exhibit remarkable attributes for sensor technology [3-4]. ZnO boasts excellent electrochemical characteristics, a large surface area, and compatibility with biological systems, while rGO offers superior electrical conductivity and chemical resilience [5]. Hence, combining these materials into a nanocomposite structure holds promise for enhancing sensor performance. Semiconductor-based nanostructured electrochemical sensors operate on the principle of converting chemical or biochemical reactions into electrical signals [6-7]. Nanoparticles with diverse nanostructures characterized by larger surface areas exhibit heightened catalytic activity and play a crucial role in environmental safeguarding. This includes air purification, energy generation, and environmental cleanup [8-9]. Previous research has underscored the versatility of ZnO nanoparticles across a spectrum of applications, spanning from solar cells and transparent conductors to photocatalysis, water treatment, and electrochemical biosensors [10].

This study introduces a ZnO_1/rGO_1 nanocomposite for use as an electrochemical sensor to measure COD in water samples. A straightforward hydrothermal method was employed to enhance the surface morphology and electrochemical activity of ZnO_1/rGO_1. The effectiveness of these electrochemical sensors was evaluated using a standard reagent, glucose analyte. Finally, the ability of ZnO_1/ rGO_1 as an electrochemical sensor for COD will be tested using real water samples. By leveraging nanotechnology and

†Paper presented at the International Conference on Advanced Materials & Sustainable Energy Technologies 2023

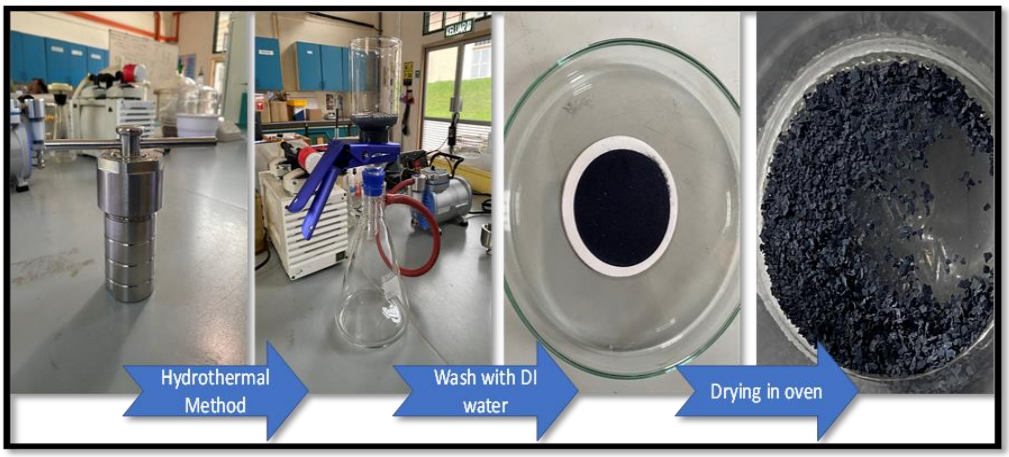

Figure 1. Process of Synthesis Material

electrochemical principles, this study offers new perspectives on the design and implementation of sensors for environmental applications. The findings presented herein contribute to the growing body of knowledge in the field of electrochemical sensing and underscore the importance of interdisciplinary research in addressing global environmental challenges.

RESEARCH METHODOLOGY

Synthesis of ZnO/rGO

Figure 1 illustrates the sequential steps involved in the synthesis process of the electrode based on ZnO. A standard procedure involved combining 10 mL of a 0.1 M solution of zinc nitrate hexahydrate ($Zn(NO_3)_2 \cdot 6H_2O$) with 10 mL of an aqueous solution of sodium hydroxide (NaOH). Consequently, this mixture was added to 50 mg of Graphene Oxide (GO) while continuously stirring for a duration of 30 minutes. The resulting mixture was transferred into Teflon-lined autoclaves and subjected to hydrothermal heating at a temperature of 180°C for a duration of 24 hours. After the chamber has cooled to room temperature, the mixture inside the reactor will be extracted. The resulting yield will be washed with deionized water and filtered using a vacuum filter. Following multiple washes, the sample will undergo a drying process in a drying oven at a temperature of 100°C for a duration of 7 hours.

Electrode Preparation

The working electrode utilized in the experiment was a glassy carbon electrode modified with ZnO_1/ rGO_1. Here, the reference electrode utilized in the experiment was an Ag/AgCl electrode immersed in a solution of 3.0 M KCl. The counter electrode, on the other hand, was a platinum rod. The experiments were
conducted under ambient temperature conditions. An ultrasonic method will be used to prepare a ZnO/ rGO-Glassy Carbon Electrode (GCE) for roughly 10 minutes. The formulation of electrode ink involves a mixture of 3 mg of the synthesized materials, 150 µL of isopropyl alcohol, 150 µL of deionized water, and 50 µL of a 5% Nafion solution by weight. The goal is to obtain a uniform suspension. Prior to utilizing the electrode, a precise amount of 2.5 µL ZnO_1/rGO_1 was meticulously deposited into the GCE surface. The electrode will then be allowed to air dry at room temperature for roughly 2 hours until the electrode is completely dried.

Electrochemical Measurements

The electrochemical studies of the synthesized materials ZnO and ZnO_1/rGO_1 sensors were evaluated in a 0.1 M NaOH background electrolyte solution containing a glucose standard analyte. This is due to explore the redox reaction involved in the electrocatalytic oxidation of this glucose molecule. The electrochemical reaction of glucose oxidation in alkaline conditions was conducted with an Autolab PGSTAT204 in a conventional three-electrode glass cell containing a modified electrode fabricated (ZnO and ZnO_1/rGO_1) set as working electrode (GCE; diameter 3 mm), Ag/AgCl as reference electrode and platinum rod as a counter electrode. This analysis will perform Cycle Voltammetric Testing with a sweep potential between +1.0 to -1.0 V. Consequently, the experiment continues with the study of the effect of scan rate from 25 to 100 mVs^{-1}. Figure 2 exhibits the overall experimental procedure for this research study.

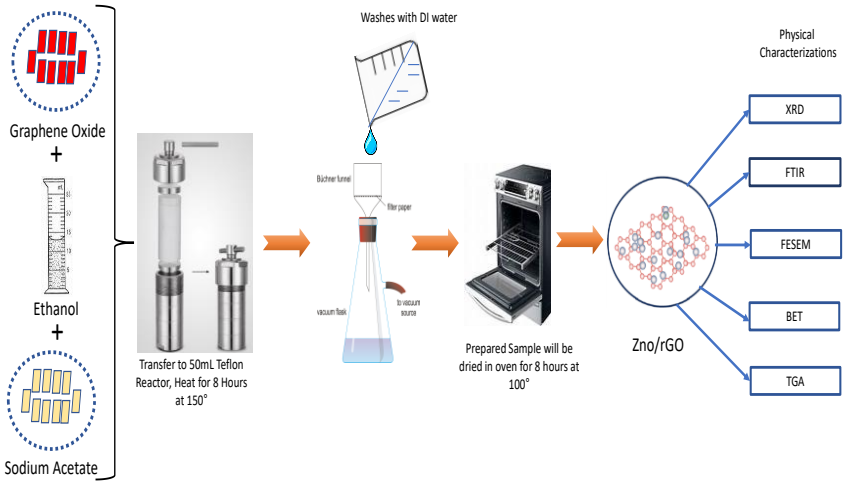

Figure 2. Overall Experimental Procedure.

Measurement of Real Waste Sample

The samples were taken from a single location in Selangor. The adjacent residential and industrial sectors were expected to have a high COD concentration. The sample was collected using a grab sampling method. The samples were kept in an icebox at a temperature of 4 °C in order to retain their original circumstances. Samples have been evaluated by both the suggested approach employing the ZnO_1/rGO_1 electrode and the HACH method (Reactor Digestion approach, Method 8000), in which digestion ranges from 0 to 1500 mg/L. The working solution was made directly in the electrochemical cell by mixing 10 mL of a real lake water sample with 0.1 M NaOH solution and homogenizing it using a magnetic stirrer. The samples were allowed to rest for approximately 5 minutes prior to measurement. The base current was measured using a 0.1 M NaOH solution. All studies were conducted at the ambient temperature (about 25°C).

RESULTS AND DISCUSSION

X-Ray Diffraction (XRD) Analysis

The X-ray Diffraction (XRD) analysis was used to examine the crystallographic structure of the synthesized sample. The existence of decreased reduced graphene oxide is indicated by a broad and low-intensity peak observed at around 24.5–27.51° in Figure 3. The XRD diffractogram of the ZnO_1/rGO_1 displays seven peaks at 32.7°, 35.2°, 37.3°, 48.6°, 57.6°, 63.8°, and 68.8°, which correspond to the (100), (002), (101), (102), (110), (103), and (112) planes, respectively. The observed peaks correspond to the JCPDS card #792205. Moreover, the XRD analysis reveals that ZnO possesses a hexagonal wurtzite crystal structure, characterized by lattice constants a=3.25 Å and c=5.207 Å. The size of the crystallites in the synthesized material was determined using Sherrer's method as stated in Equation (1):

$$d\ (Å) = K\lambda/\beta \cos\theta, \quad (1)$$

where λ is the employed X-ray wavelength (1.5406 Å), β is the Full Width at Half Maximum (FWHM) of a specific peak, and K is the form factor, which typically takes a value of 0.9. A crystallite size of 17.82 nm was observed for the (101) plane. In practically every respect, the XRD pattern that was produced for ZnO_1/rGO_1 is the same as that of ZnO. The ZnO_1/rGO_1 composite contains no discernible impurities, as evidenced by the similarity in the XRD pattern, and the hexagonal structure of ZnO remains unaffected by the inclusion of graphene. [11]. This also demonstrates that the existence of rGO does not affect the structure of ZnO particles. The disappearance of the GO signals shows that GO has been completely exfoliated as a result of the insertion of ZnO particles.

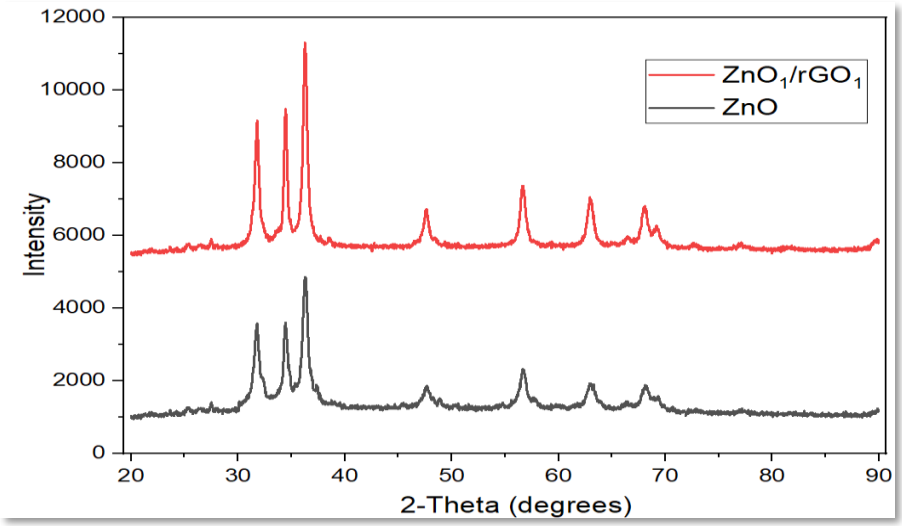

Figure 3. XRD diagrams for ZnO and ZnO_1/rGO_1.

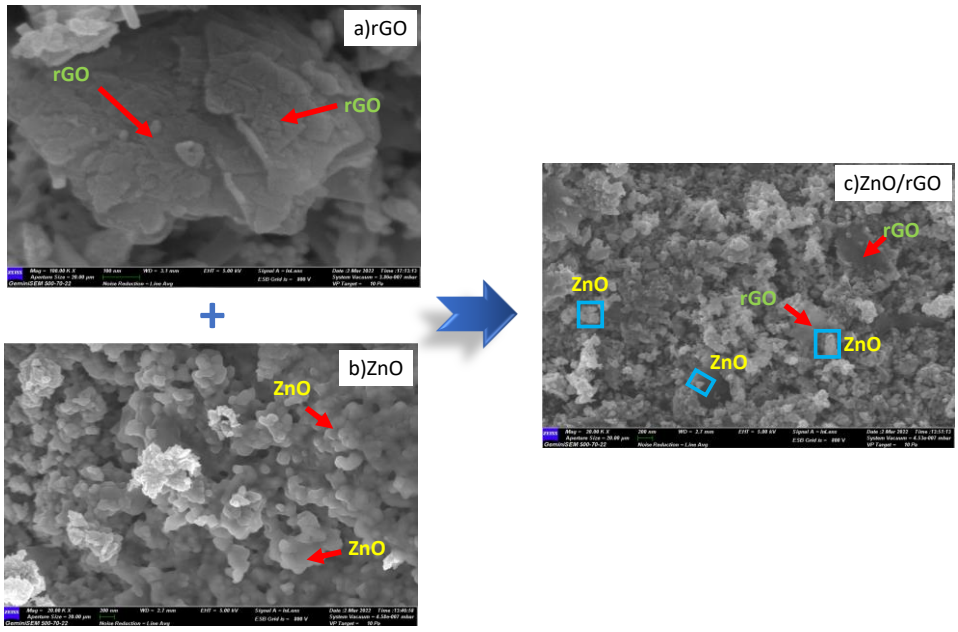

Figure 4. FESEM pictures of: (a) rGO, (b)ZnO and (c) ZnO_1/rGO_1.

Field Emission Scanning Electron Microscopy (FESEM)

The FESEM images presented in Figure 4 illustrate the morphological characteristics of rGO, ZnO, and rGO/ZnO nanomaterials, respectively. Figure 5(a) depicts an irregular and well-organized multilayer structure of rGO in a pure rGO sample. On the other hand, Figure 4(b) portrays the accumulation of particles, with particles estimated to be approximately 100 nm in size. These morphological and size variations may be caused by alterations in the ZnO nucleation and growth process. The aggregation of ZnO nanoparticles results in a greater average diameter size in the pure sample than in the composite [10]. The synthesized materials' FESEM images, displayed in Figure 4(c), obviously demonstrate ZnO's anchoring to rGO. Compared to pure ZnO materials, there is less aggregation of particles in the composite when rGO is present because ZnO nanoparticles adhere to it by interacting with remaining functional groups [12].

Fourier-Transform Infrared Spectroscopy (FT-IR)

Fourier-Transform Infrared Spectroscopy (FT-IR) analysis was conducted on fabricated nano-particles to pinpoint the unique functional groups associated with them. Note that the detected peaks in the spectrum indicate the existence of

these functional groups within the nanoparticles. Figure 5 illustrates a band between 400-500 cm^{-1}, revealing the stretching mode and confirming the formation of Zn-O bonds [11]. The FT-IR spectra of the synthesized materials indicate absorption peaks ranging from 4000 to 400 cm^{-1}. Specifically, the peak at 480 cm^{-1} serves as a distinctive marker for the Zn-O bond, thereby confirming the existence of ZnO in the nanocomposite. The stretching modes of the acetate group manifest in absorption peaks ranging from 1350 to 1600 cm^{-1} (–COOH). Note that the absorption peak at 1115 cm^{-1} indicates the presence of Carbon-Oxygen (C-O) bonds, whereas stretching peaks at 2950 and 2850 cm^{-1} reveal the presence of Carbon-Hydrogen (C-H) bonds [13]. The investigation of the GO spectrum indicates the existence of bands linked to C–O at 1048 cm^{-1}, C–O–C at 1223 cm^{-1}, C–OH at 1376 cm^{-1}, and C=O in carboxylic acid and carbonyl groups. These bands are mainly discovered along the edges of the graphene sheets and can also be observed on the basal plane. Additionally, there is a wide peak between 3000 and 3500 cm^{-1} which corresponds to O–H [14].

Brunauer-Emmett-Teller (BET) Adsorption Desorption Analysis

The findings of BET adsorption-desorption studies conducted to evaluate the physical adsorption of gas on the surface areas of both pure ZnO and ZnO_1/rGO_1 nanocomposite materials are shown in Figure 6. Significantly, the desorption branch does not reach the adsorption branch, suggesting a kinetic activity problem that is likely caused by the presence of micropores. Hence, it confirms the presence of pore space that has a dimension of less than 1 micro [15]. Both ZnO and ZnO_1/ rGO_1 nanocomposite demonstrate significant adsorption when the relative pressure (P/P0) approaches 1.0, suggesting the presence of large mesopores and macro-pores [16]. This discovery is additionally corroborated by the pore-size distribution analysis, which spans from 2 to 80 nm.

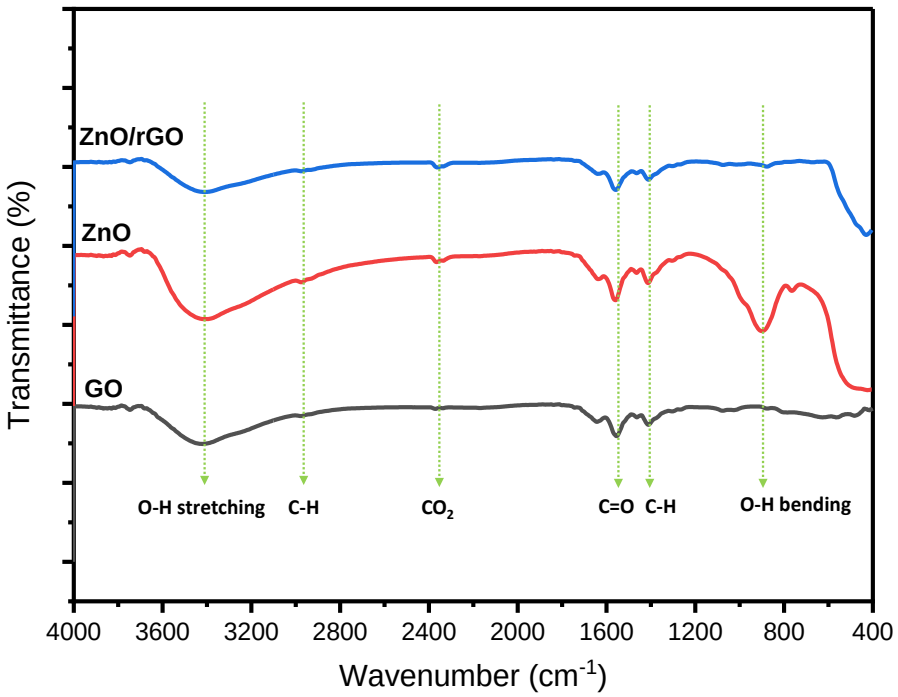

Figure 5. FTIR spectrum for GO,ZnO and ZnO_1/rGO_1.

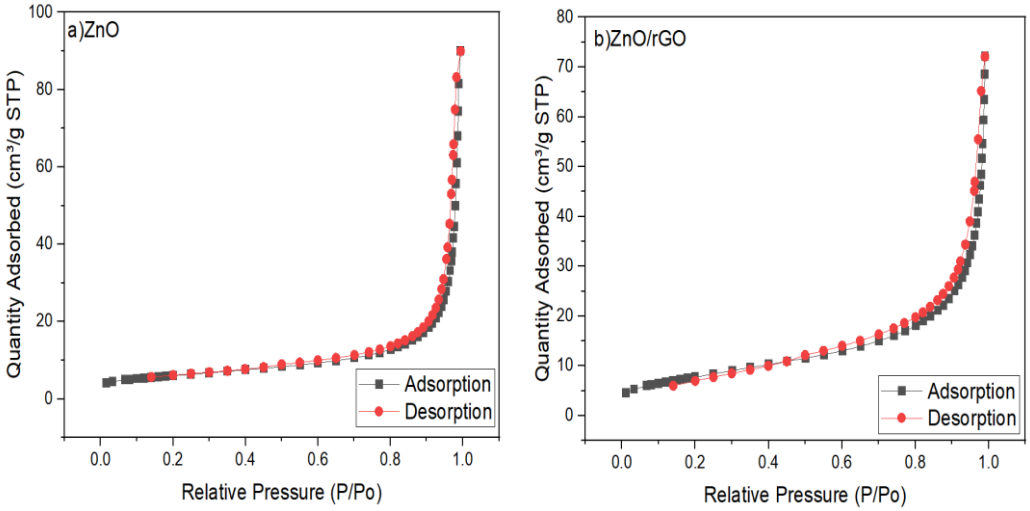

Figure 6. BET Curves for a) ZnO and b) ZnO_1/rGO_1.

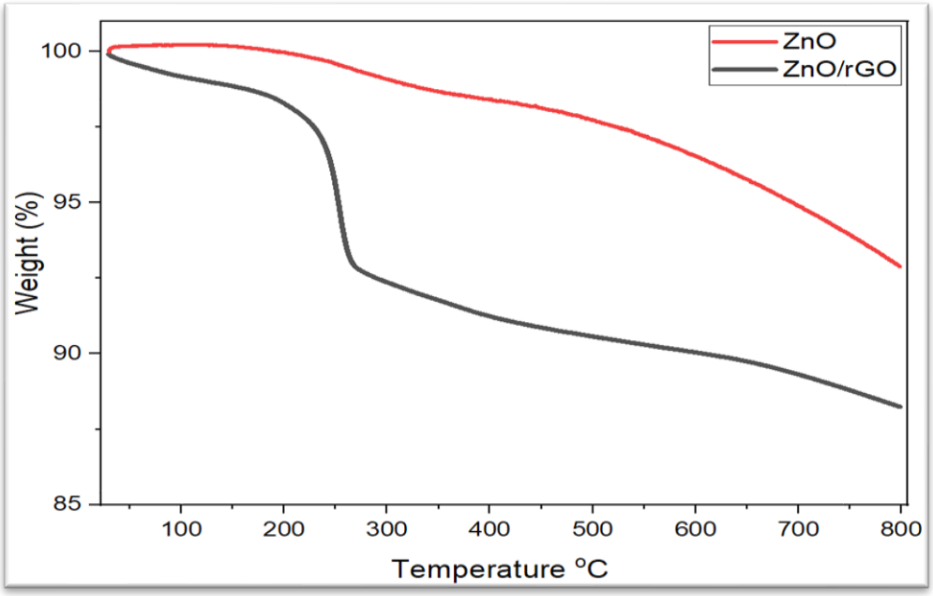

Figure 7. TGA Curves for ZnO and ZnO_1/rGO_1.

Thermal Gravimetric Analysis (TGA)

Figure 7 illustrates the Thermogravimetric and Derivative Analysis (TGA/DTA) curves of the ZnO and ZnO_1/ rGO_1 materials developed using the hydrothermal technique. The heating procedure started at a temperature of 50°C and increased to 800°C at a pace of 10°C per minute. Both the TGA curves of ZnO and ZnO_1/rGO_1 composites exhibit a decrease in weight from ambient temperature to 250°C, which is likely due to the removal of water molecules attached to the surface. From 250°C to 800°C, the decrease in weight can be attributed to the removal of oxygen-containing groups and the breakdown of the carbon framework in the synthesized material [17]. This thermal research offers an important understanding of how the chemical structure and durability of the synthesized materials when subjected to different temperature conditions.

Cyclic Voltammetric Studies

In alkaline environments, ZnO_1/rGO_1 particles exhibit electrocatalytic activity, facilitating the oxidation of various organic compounds, which are often the principal contributors to the chemical oxygen demand (COD) in water samples. To assess the electrochemical efficacy of the ZnO_1/rGO_1 electrode, cyclic voltammetry was conducted across a potential range from -0.8 to +0.4 V. The cyclic voltammogram depicted in Figure 8 illustrates the typical current-voltage behavior observed at both synthesized materials in a 0.1 M NaOH solution. The first anodic peak (Peak 1) at -0.38 V vs. Ag/AgCl represents the creation of the initial layer of

Zinc (I) Oxide. In comparison, the larger Peak 2 at -0.11 V vs. Ag/AgCl represents the formation of a second mixed layer of Zn(II) Oxide and Zn(II) Hydroxide (ZnO/Zn $(OH)_2$). The 0.70 V vs. Ag/AgCl value indicates that Zn(II) has been oxidized to Zn(III).

Upon closer examination during the reverse scan, cathodic peaks (Peaks 3 and 4) emerge, corresponding to the reduction reactions of Zn(II) to Zn(I) at -0.55 V vs. Ag/AgCl and Zn(I) to Zn(0) at -0.84 V vs. Ag/AgCl, respectively. This electro-chemical behavior is notably influenced by the concentration of hydroxide ions and the prior formation of specific Zn(II) oxide layers. Moreover, the involvement of Zn(III) species as electron-transfer mediators has been proposed to elucidate the superior performance of ZnO_1/rGO_1 electrodes in alkaline environments, particularly in anodic processes involving various organic compounds. Additionally, the stable modification of the ZnO_1/rGO_1 on the surface of the GC electrode is evidenced by the absence of significant peak current fluctuations across 20 consecutive cycles, suggesting its suitability for COD measurement applications.

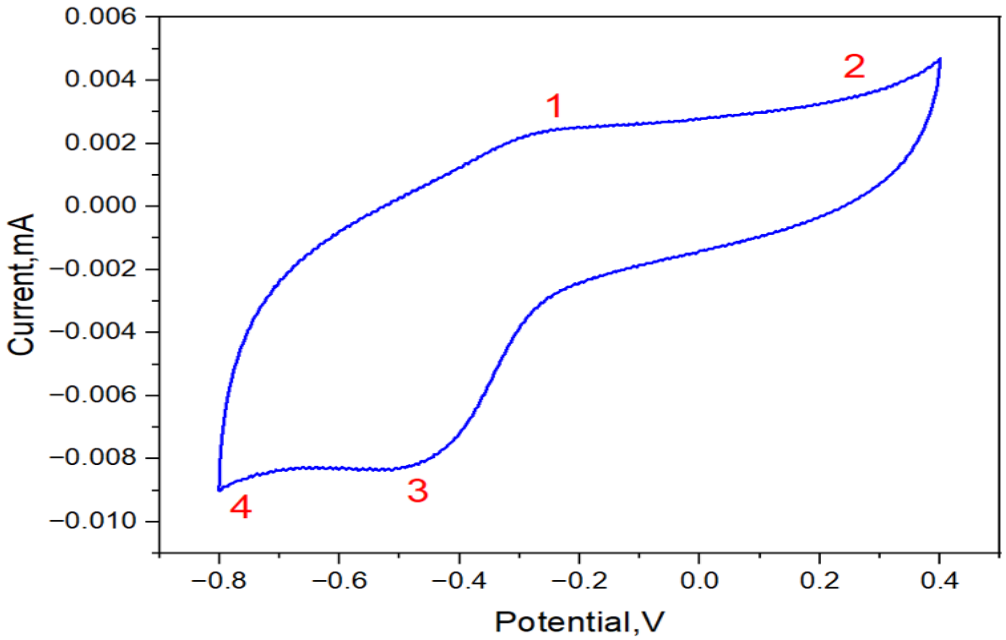

Figure 8. CV curve of ZnO_1/rGO_1 electrode in 0.1M NaOH solution.

Response of Different Electrodes Towards Glucose

As mentioned earlier, both ZnO and ZnO/rGO electrodes were employed to measure oxidation currents in various glucose solutions, serving as benchmarks for COD determination. Figure 9 displays cyclic voltammograms obtained during the oxidation of glucose at different concentrations. As depicted in the figure, the oxidation current signals at ZnO and ZnO/rGO electrodes exhibit linear increments with rising COD concentrations. This observation underscores the potential of these electrodes for accurately assessing COD levels in solutions containing glucose. The ZnO electrocatalytic reaction with organic is explained through the reaction mechanism below:

$$Zn + 2OH^- \rightarrow Zn(OH)_2 + 2e^- \quad (2)$$

$$Zn(OH)_2 + OH^- \rightarrow Zn(III)OOH^* + H_2O + e^- \quad (3)$$

The Zn (III) species formed at the electrode surface (Equation 2) rapidly oxidizes organic compounds (Equation 4), producing Zn (II) and sacrificing Zn (III) as follows,

$$Zn(III)OOH^* + Organics_{(red)} + H_2O \rightarrow Zn(OH)_2 + Organics_{oxi} + OH^- \quad (4)$$

The potential involvement of both Zinc (II) and Zinc (III) in the oxidation reactions of organic compounds is plausible, given their presence within this specific potential range [18]. Notably, the peak current recorded at -0.20 V demonstrates a linear correlation with the chemical oxygen demand (COD) values. It calculates through the theoretical oxidation of glucose according to Equation 4, within the concentration range of 158.0 to 540 mg/L COD (as illustrated in Figure 9). On the other hand, figure 10 presents the calibration curves, depicting the relationship between peak current and glucose concentration across various electrodes. Over the glucose concentration range of 158 to 540.0 mg/L, a strong linear relationship is evident in the oxidation current. Table 1 summarizes

the fitting curves, each electrode's linear correlation coefficient, and the detection limit.

Comparative analysis against electrochemical COD sensors utilizing both synthesized materials reveals that the ZnO_1/rGO_1 modified electrode exhibits a lower detection limit and higher sensitivity. This underscores the enhanced performance of the ZnO with the present of rGO in detecting and quantifying COD levels, presenting promising prospects for its application in environmental monitoring and analysis. The rGO improve the performance of ZnO as electrochemical sensor by offering a large surface area, excellent electron transfer capability, and a biocompatible platform, surface-rich functional groups can assess a variety of biomarkers.

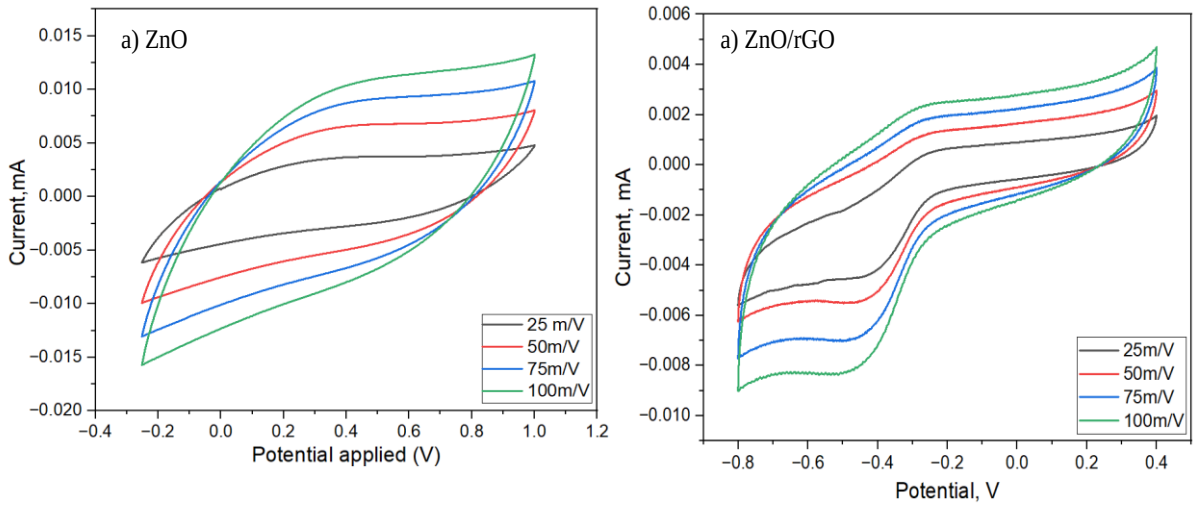

Figure 9. CV curves a) rGO, b) ZnO and c) ZnO_1/rGO_1 at different scan rate.

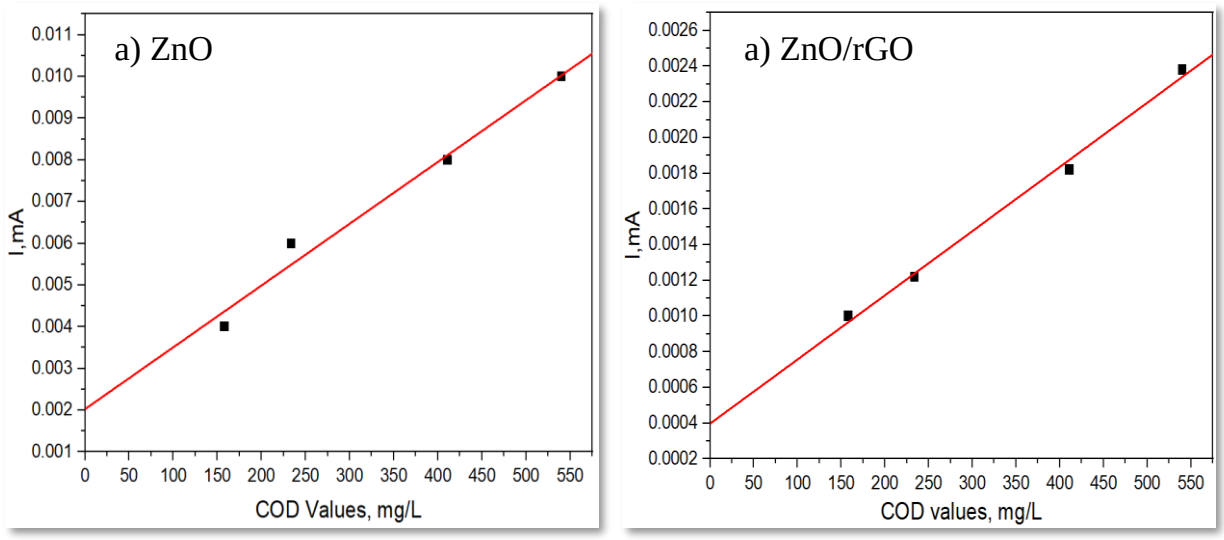

Figure 10. Calibration chart displays the present signal, ΔIpa, for both ZnO and ZnO_1/rGO_1, as it varies with COD levels.

Table 1. Summary performance of detection limit of each electrode.

Electrode	Calibration Curve	Linear Correlation Coefficient	Detection Limit (mg/L)
ZnO	$1.48 \times 10^{-3}\,[\mathrm{COD}]\left(^{\mathrm{mg}}/_{\mathrm{l}}\right) + 0.00203$	0.9898	3.3 SD/Slope= 1.0
ZnO_1/rGO_1	$3.60 \times 10^{-4}\,[\mathrm{COD}]\left(^{\mathrm{mg}}/_{\mathrm{l}}\right) + 3.98 \times 10^{-4}$	0.9973	3.3 SD/Slope= 0.513

Table 2. The COD results of real lake water samples were compared using the ZnO_1/rGO_1 modified electrode and the standard dichromate methodology.

Material	No Sample	COD electrode	RSD%	COD standard method	RSD%
ZnO_1/rGO_1	1	37.78 ± 5.0	3.61	40.0 ± 5.0	3.54
	2	38.81 ± 5.0	3.83	39.5 ± 5.0	3.58
	3	39.78 ± 5.0	3.56	40.8 ± 5.0	3.24

Determination of COD in Real Sample

A single water sample was obtained from Lake Water to assess the feasibility of utilizing this sensor for monitoring COD levels in a water treatment facility. The COD concentration of the lake water sample was determined using the electrochemical testing method using synthesized material and compared with values obtained through traditional COD analysis. Results are presented in Table 2, indicating that COD values obtained via the electrochemical method fall within ±10% of those determined by establish method. Each water sample underwent three parallel measurements, yielding consistent results that align with those obtained using the standard method approach. Mean value of COD 35-40 mg/l during dry season. By National Water Quality Standard (NWQS), it was found that COD concentration is in class III which Department of Environment prescribed limit is at 50 mg/l. The lake had received a lot of sources of contamination that might be coming from the industrial, residential area and agricultural activities surrounding the lake which release toxic waste and require a lot of oxygen to oxidize the organic materials. In addition, low flow of water makes difficult to oxidation process.

CONCLUSION

The primary aim of this project was to explore cost-effective and efficient techniques for synthesizing ZnO_1/rGO_1 nanocomposites suitable for industrial applications in producing fine powders with uniform particle shapes. To achieve this goal, we utilized the most economical starting materials available. The hydrothermal method successfully synthesized the ZnO_1/rGO_1 composite, confirmed through XRD, FTIR, FESEM, BET, and TGA analyses. XRD results demonstrated that the ZnO_1/rGO_1 nanocomposite maintained the hexagonal wurtzite structure of ZnO, indicating no structural alteration upon rGO incorporation. FESEM imaging revealed ZnO nanoparticles predominantly forming nanosphere morphologies with minimal agglomeration, while distribution of ZnO nanosparticles on the rGO surface indicated prevention of ZnO particle aggregation by rGO. The fabricated sensors ZnO and ZnO_1/rGO_1 electrodes exhibited detection limits of approximately 1.0 mgL^{-1} and 0.50 mgL^{-1}, respectively, facilitating COD analysis in surface water. These results closely aligned with the standard COD method, underscoring the potential of the prepared sensors for routine analysis of real lake water samples. This study highlights the promising advancements in electrochemical sensors surveillance of the environment, with potential applications extending to biomedical and food processing quality control areas.

ACKNOWLEDGEMENT

Authors acknowledge the Ministry of Higher Education (MOHE) for funding under the Fundamental Research Grant Scheme (FRGS)(FRGS/1/2021/TK0/UNIKL/02/8).

REFERENCES

1. Boguniewicz-Zablocka, J., Klosok-Bazan, I., Naddeo, V. andMozejko, C. A. (2020) Cost-effective removal of COD in the pre-treatment of wastewater from the paper industry. *Water Sci. Technol.*, **81(7)**, 1345–1353.

2. Ullah, Z. and Zeshan, S. (2020) Effect of substrate type and concentration on the performance of a double chamber microbial fuel cell. *Water Sci. Technol.*, **81(7)**, 1336–1344.

3. Ramamurthi, N. K. K. (2020) Synthesis of ZnO /rGO nanocomposites by wet impregnation method for photocatalytic performance against RhB dye and 4 - chlorophenol under UV light irradiation. *J. Mater. Sci. Mater. Electron.*, 0123456789.

4. Akilarasan, M., Kogularasu, S., Chen, S. M., Chen, T. W. and Lin, S. H. (2018) One-step synthesis of reduced graphene oxide sheathed zinc oxide nanoclusters for the trace level detection of bisphenol A in tissue papers. *Ecotoxicol. Environ. Saf.*, **161**, April, 699–705.

5. Rodwihok, C., Wongratanaphisan, D., Linh, Y. and Ngo, T. (2019) Effect of GO Additive in ZnO/rGO Nanocomposites with Enhanced Photosensitivity and Photocatalytic Activity.

6. Kour, R., Arya, S., Young, S. -J., Gupta, V., Bandhoria, P. and Khosla, A. (2020) Review—Recent Advances in Carbon Nanomaterials as Electrochemical Biosensors. *J. Electrochem. Soc.*, **167(3)**, 037555.

7. Li, Z., *et al.* (2019) Application of electrochemical aptasensors toward clinical diagnostics, food, and environmental monitoring: Review. *Sensors (Switzerland)*, **19**, 24,

8. Wang, M., *et al.* (2018) Fabrication of a novel ZnO–CoO/rGO nanocomposite for nonenzymatic detection of glucose and hydrogen peroxide. *Ceram. Int.*, **44(5)**, 5250–5256.

9. Agnihotri, A. S., Varghese, A. and N. M. (2021) Transition metal oxides in electrochemical and bio sensing: A state-of-art review. *Appl. Surf. Sci. Adv.*, **4**, February.

10. Wang, Z., Li, H., Tang, F., Ma, J. and Zhou, X. (2018) A Facile Approach for the Preparation of Nano-size Zinc Oxide in Water / Glycerol with Extremely Concentrated Zinc Sources, 1–9.

11. Thongam, D. D., Gupta, J. and Sahu, N. K. (2019) Effect of induced defects on the properties of ZnO nanocrystals: surfactant role and spectroscopic analysis. *SN Appl. Sci.*, **1(9)**, 1–14.

12. Ashraf, M. A., Peng, W., Zare, Y. and Rhee, K. Y. (2018) Effects of Size and Aggregation/ Agglomeration of Nanoparticles on the Interfacial/ Interphase Properties and Tensile Strength of Polymer Nanocomposites.

13. Bano, N., Hussain, I., EL-Naggar, A. M. and Albassam, A. A. (2019) Reduced graphene oxide nanocomposites for optoelectronics applications. *Appl. Phys. A Mater. Sci. Process.*, **125**, 3, 0.

14. Ravi, K., *et al.* (2018) ZnO/RGO nanocomposite via hydrothermal route for photocatalytic degradation of dyes in presence of visible light. *Int. J. Chem. Stud.*, **6(6)**, 20–26.

15. Moussa, H., Girot, E., Mozet, K., Alem, H., Medjahdi, G. and Schneider, R. (2016) ZnO rods/ reduced graphene oxide composites prepared via a solvothermal reaction for efficient sunlight-driven photocatalysis. *Appl. Catal. B Environ.*, **185**, 11–21, December, 2015.

16. Lim, A., Chew, J. J., Ngu, L. H., Ismadji, S., Khaerudini, D. S. and Sunarso, J. (2020) Synthesis, Characterization, Adsorption Isotherm, and Kinetic Study of Oil Palm Trunk-Derived Activated Carbon for Tannin Removal from Aqueous Solution. *ACS Omega*, **5(44)**, 28673–28683.

17. Arif, D., Hussain, Z., Sohail, M., Liaqat, M. A., Khan, M. A. and Noor, T. (2020) A Non-enzymatic Electrochemical Sensor for Glucose Detection Based on Ag@TiO2@ Metal-Organic Framework (ZIF-67) Nanocomposite. *Front. Chem.*, **8**, October, 1–8.

18. Fernández-garcia, M. J. A. and Rodriguez (2007) Metal Oxide Nanoparticles. *Nanomater. Inorg. Bioinorg. Perspect.*, **60**, October.